COBEM 2023 27TH INTERNATIONAL CONGRESS OF MECHANICAL ENGENEERING

ABCM Brazilian Society of Mechanical Sciences and Engineering
27th ABCM International Congress of Mechanical Engineering
December 04-08, 2023, Florianópolis-SC, Brazil

COB-2023-0155

PLASMA-ASSISTED AND FURNACE PYROLYZED POLYSILAZANE-BASED CR-SI-C-N COMPOSITE COATING SYSTEM – A COMPARISON

Daniel Auri Schaefer
Tatiana Bendo
Aloisio Nelmo Klein

Federal University of Santa Catarina, Mechanical Engineering Department, Materials Laboratory (LABMAT), BR-88040-900, Florianópolis, Brazil
daniel.as@labmat.ufsc.br
tatiana.bendo@labmat.ufsc.br
a.n.klein@ufsc.br

Abstract. *Coatings based in polymer-derived ceramics (PDCs) have gained attention due to their properties like easy application on metallic substrates of any shape, low-temperature processing, and the potential to tailor the properties via microstructure and composition design. Furthermore, these compounds possess outstanding protective properties that are necessary for environmental barrier applications. In this work, a PDC coating loaded with reactive Cr fillers was applied by spray coating on a sintered steel substrate and subsequently pyrolyzed through conventional furnace pyrolysis (CFP) and plasma-assisted pyrolysis (PAP). The sample substrate and resulting layer system were characterized by optical and scanning electron microscopy, energy-dispersive spectrum, and X-ray diffraction. The interaction of reactive plasma atmosphere with polymeric ceramic precursor and Cr reactive filler led to the formation of an adherent and dense coating. The X-ray diffractograms exhibited the formation of a mixed hexagonal β-Cr_2N and cubic CrN phases, with higher intensity peaks related to the cubic phase at the CFP process and of hexagonal phase at the PAP process, involved by an amorphous SiCN matrix. A dense reaction zone is visible at the coating/steel interface, indicating good bonding. This region is thicker in samples processed via PAP, indicating higher interdiffusion between species.*

Keywords: *Polymer-derived Ceramic, Plasma-Assisted Pyrolysis, Cr-Si-C-N coating, ceramic coating.*

1. INTRODUCTION

New technologies for protection against corrosion applications are always in demand and are a great challenge for several fields of the industry. Generally, the triggering of corrosive processes results in the replacement of parts, which generates high costs, environmental issues, and high energy consumption.

Rather than designing new structural materials that can sustain harsh environmental conditions, the combination of conventional metals and coatings with tailored properties is usually a technologically simpler and economically more interesting approach. In this scenario, protective coatings made on non-oxide and/or oxide PDCs (polymer-derived ceramics) are potential materials to improve the resistance to corrosion of metals, due to their superior properties in severe environments and synergy with the metal surface.

Preceramic polymers are mainly silicon-containing organic/inorganic polymers, forming amorphous ceramics after pyrolysis at temperatures between 600 and 1000 ºC. PDCs are easy to apply on substrates of any shape by dip coating, spray-coating, spin-coating, or tape casting. The main drawback of the PDC technology is the unavoidable shrinkage that occurs during pyrolysis, due to the large density change when the preceramic polymer is converted into a ceramic product (Riedel et al. 2006), (Colombo et al. 2010). The volume shrinkage can be greater than 50 %, and to control this shrinkage, the precursor can be loaded with active or passive fillers. The active fillers can react with pyrolysis atmosphere and/or decomposition products from the polymer precursor, generating new phases with increased specific volumes, while the passive fillers do not undergo any chemical reaction nor mass and volume change during pyrolysis (Greil, 1995). Suitable precursor and filler system choices, in combination with pyrolysis atmosphere and processing parameters, are of fundamental importance to manufacturing tailored PDC coatings for engineering components.

Among the broad variety of protective coatings, CrN-based coatings are well known for their protective properties against wear, erosion, oxidation, and corrosion. The addition of silicon (Si) and carbon (C) to the CrN coatings leads to improvement of the mechanical and oxidation properties (Cai et al. 2010), (Cai, Huang and Yang, 2015), (Gilewicz et al. 2016), (Hatakeyama et al. 2022), (Lin et al. 2013), (Lin et al. 2016), (Wang et al. 2015a), (Wang et al. 2015b), (Wang et al. 2019), (Wu et al. 2016).

In this work, Plasma-assisted Pyrolysis (PAP) is used to process PDC-loaded ceramic coatings on a sintered steel substrate. Aiming to improve both coating and steel surface properties, new ceramic phases are expected to be formed during the conversion process of the Cr-Si-C-N system studied. Results are presented in terms of microstructure, crystalline phases, and chemical composition of the coatings, substrates, and coating-substrate interfaces.

2. EXPERIMENTAL PROCEDURE

2.1 Sintered substrate and coating mixture

The steel substrates were processed following the conventional powder metallurgy route: mixing of powders, die compaction of the powder mixture, and conventional furnace sintering performed at controlled atmosphere. The powders used in this study were 97.4 wt.% of pre-alloyed Fe1.5Mo (AstaloyMo, Höganäs), 2.0 wt.% of pure nickel (Epson Atmix), 0.6 wt.% of graphite (Nacional Grafite) and 0.8 wt.% of amide wax lubricant. The subsequent steps including the sintering step are described elsewhere (Martins et al., 2020).

For this study, coatings based on polysilazanes were prepared with the commercially available liquid poly(organo)silazane DURAZANE 1800 (Merck KGaA) as a preceramic polymer. The experimental procedure for the preparation of the coating suspensions can be divided into different steps: at first, the dispersant DISPERBYK-2070 (BYK-Chemie GmbH) was dissolved in di-n-butyl ether (purity >99%, Alfa Aesar GmbH & Co KG). Then Cr powder with particle size $d_{90} < 8.0$ µm (purity >99 %, Alfa Aesar GmbH & Co KG) was added and dispersed by ultrasound and mechanical stirring. In a third step, the silazane was added to the suspension and mixed by mechanical stirring. To accelerate the crosslinking reaction of the preceramic polymer, 3 wt% DCP (dicumyl peroxide, Sigma–Aldrich Chemie GmbH), was dissolved in the pure liquid precursor prior to the addition to the suspension.

The Cr powder was chosen as an active filler because of its high-volume increase by forming CrN when reacting with N_2 atmosphere (Greil, 1995).

The final suspension, with the composition of the topcoat, was applied by spray coating with an automatic spray-coater (Mignon 3, Krautzberger), deposition speed of 50 mm s^{-1}, and 100 mm distance to the sintered steel substrate. Mixtures with different proportions of precursor and Cr powder were prepared, deposited on the substrate, and then pyrolyzed in a conventional furnace (under the same parameters as conventional pyrolysis, used throughout the work).

The pyrolyzed surfaces were analyzed for the number of defects, such as high porosity, cracks, shrinkage, and adhesion. Based on these results, the best precursor-to-filler ratio was 45 % (HTT1800 + DCP) and 55 % (Cr powder – active filler) in volume percentage, which was used for the development of this study.

Figure 1 presents a sequential diagram of the sample production process, including the production of suspensions (precursor and active filler), application, and pyrolysis.

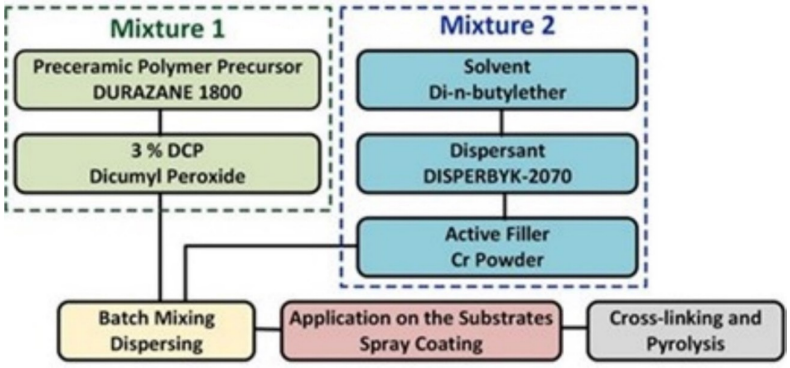

Figure 1. - Schematic flowchart of the processing route for the polymer-derived ceramic coatings.

2.2 Conventional Furnace Pyrolysis (CFP) and Plasma-Assisted Pyrolysis (PAP)

CFP and PAP were performed at the same temperature, using a heating rate of 3 $^{\circ}$Cmin^{-1} up to 1000 °C and kept at this temperature for 1 h, under a nitrogen atmosphere. The CFP process was performed in a tubular furnace (RO 10/100, Heraeus). The PAP experiments were performed in a hybrid plasma reactor, which basically consists of a cathode connected to a negative voltage output and a grounded anode, besides a resistive heating system inside the vacuum chamber. Details of the hybrid plasma reactor setup are described elsewhere (Seifert et al., 2016), (Martins et al., 2020). For the PAP process, the samples were placed in the cathode configuration to allow a higher energetic interaction of the coating with reactive species of the plasma. The anode was grounded, and the cathode was negatively biased, using a DC pulsed power source with an output voltage of 500 V. For both CFP and PAP, the temperature was measured using a

reference sample with a type-K thermocouple inside, positioned symmetrically with the specimens. All the treatments were carried out under a reduced nitrogen pressure of 200 Pa (purity 99.99 %) and a flowing rate of 4.17×10^{-6} m^3s^{-1}.

2.3 Characterization methods

The microstructure of the pyrolyzed composite coatings and steel substrate were analyzed using a scanning electron microscopy (SEM - VEGA3 TESCAN) equipped with an energy dispersive X-ray (EDX) apparatus (OXFORD Instruments). To follow the weight changes during the pyrolysis, the active filler (Cr powder), the precursor (Durazane 1800 + DCP), and the composite (precursor + Cr) were analyzed with thermal gravimetric analysis (TGA - L91, Linseis) up to 1000 °C with a heating rate of 3 $^{\circ}Cmin^{-1}$ under a nitrogen atmosphere (purity 99.9 %). To identify the crystalline phases of composite coatings, X-ray diffractograms were recorded from the surface of samples using a D8 Advance diffractometer (Bruker AXS) with CuK_{α} radiation source by employing the Bragg-Brentano geometry. The phases from the diffraction peak positions were identified using the JCPDS database as a reference.

3. RESULTS AND DISCUSSION

Figure 2a presents the mass increase behavior obtained for the Cr powder in nitrogen atmosphere. The Cr powder presented a high mass increase starting around 600 °C. As reported in the literature, a direct combination between Cr and N_2 to form CrN occurs at 800 °C, following the reaction $2Cr + N_2 \rightarrow 2CrN$ (Šajgalík, Lenčéš and Hnatko, 2010). According to the reaction equation, the complete conversion of Cr into CrN represents a mass increase of approximately 27 wt.%. The thermogravimetric analysis indicates a maximal mass increase of almost 27 wt.%, obtained after 2 hours at 1000 °C. This result may indicate that there is a strong tendency for all Cr particles to be converted to CrN during pyrolysis under those conditions.

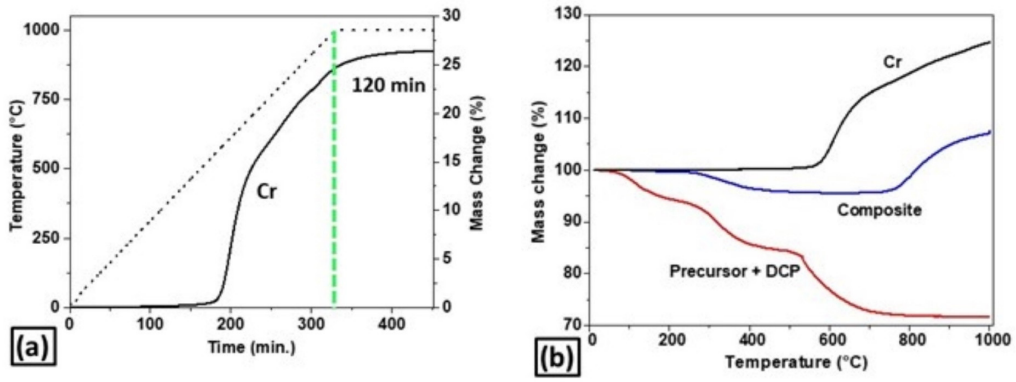

Figure 2. TGA obtained in nitrogen atmosphere for: (a) Cr powder (active filler) held for 2 hours at 1000 °C - the final temperature, (b) precursor + DCP, Cr powder, and the composite mixture – precursor + active filler.

Fig. 2b presents the thermal gravimetric analysis (TGA) of the selected materials, the active filler (Cr powder), the preceramic polymer with the addition of 3 wt.% DCP and the precursor + active filler mixture (precursor-to-filler ratio 45:55). All curves were obtained at nitrogen atmosphere.

Global mass loss of about 28 wt. % was observed for the pyrolysis of the precursor + DCP up to 1000 °C in nitrogen atmosphere. The TGA curve for precursor + DCP (Fig. 2b) consists of three different regions whose behavior is well-known in the literature (Motz, Schmidt and Beyer, 2008), (Flores et al. 2013). The first region, up to approximately 300 °C, shows no significant mass loss, which is related to the cross-linking process, in this case, assisted by the use of DCP that acts by reducing the onset temperature and the evaporation of lighter molecules. Thereabout 300 and 700 $^{\circ}C$ the largest mass loss occurs leading to an organic-to-inorganic transformation, from a thermoset polymer precursor into a ceramic material. At temperatures higher than 700 $^{\circ}C$, the polymer system was almost completely destroyed and at 1000 $^{\circ}C$ the conversion into ceramic is complete.

As expected, the mixture, precursor + Cr powder (Fig. 2b) shows a mass increase, confirming the active filler behavior. The mass increase starts at about 800 $^{\circ}C$, which is the temperature where CrN formation occurs. At 1000 $^{\circ}C$ the mass increase reaches approximately 9 %. This value is lower than expected and may be related to the formation of other possible phases and the incomplete conversion of filler particles.

Figure 3 presents the XRD patterns of the crystalline phases identified in the Cr powder as received and after TGA analysis in N_2 atmosphere, and in the surface of coatings after CFP and PAP processes. The process was performed at 1000 $^{\circ}C$, during 2 h for TGA and 1 h for CFP and PAP.

After TGA analysis of the Cr powder, only the cubic CrN phase was detected, which corroborates the behavior observed for the mass change in Figure 2(a). For the composites, at the pyrolysis temperature of 1000 ˚C performed in the plasma reactor, the phases Cr_2N (PDF 00-035-0803) and CrN (PDF 00-011-0065) were detected, with the majority phase being Cr_2N. After CFP, unreacted active filler was still detected on the coating surface in addition to the Cr_2N and CrN phases, where the most intense peaks were from the CrN phase. When the highly energetic species of the plasma atmosphere (especially atomic nitrogen) interact with the Cr filled PDC coating, the chemical potential of the system is modified when compared with the traditional process, where there is only molecular nitrogen (N_2). The energetic nitrogen radicals present in the PAP atmosphere, and its associated physical-chemical activity, increase the reactivity of the filler conversion favoring the formation of Cr_2N at elevated temperatures (Wierzchon, Ulbin-Pokorska and Sikorski, 2000).

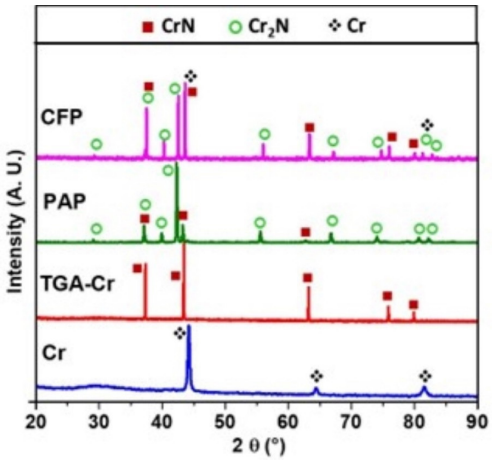

Figure 3. XRD spectra of Cr powder as received and after TG analysis (TGA-Cr), after conventional furnace pyrolysis (CFP), and after plasma-assisted pyrolysis (PAP).

Scanning electron micrographs of the surface of the coating, obtained after pyrolysis at temperatures of 1000 ˚C of both CFP and PAP processes, are presented comparatively in Figure 4. It can be observed different morphologies between CFP (Figure 4(a)) and PAP (Figure 4(b)). After treatment in plasma, the coating particles seem more coalesced, less rough and the surface presents much less porous when compared with the conventional furnace process. As reported in the literature, the active species of the plasma treatment (e.g., radicals, ions, and electrons) can induce physical and chemical modifications to the surface of materials that strongly influence their macroscopic response. Moreover, when samples are placed on the cathode (negatively polarized), the mass transport mechanisms and condensation of atoms on the sample surface are activated, as a consequence of ion bombardment (Chapman, 1980). Regarding the microstructure of the layers, these plasma characteristics are responsible for the denser and more coalesced microstructure observed in PAP, a similar result to the ones found in previous studies of our group (Seifert et al. 2015), (Martins et al. 2020).

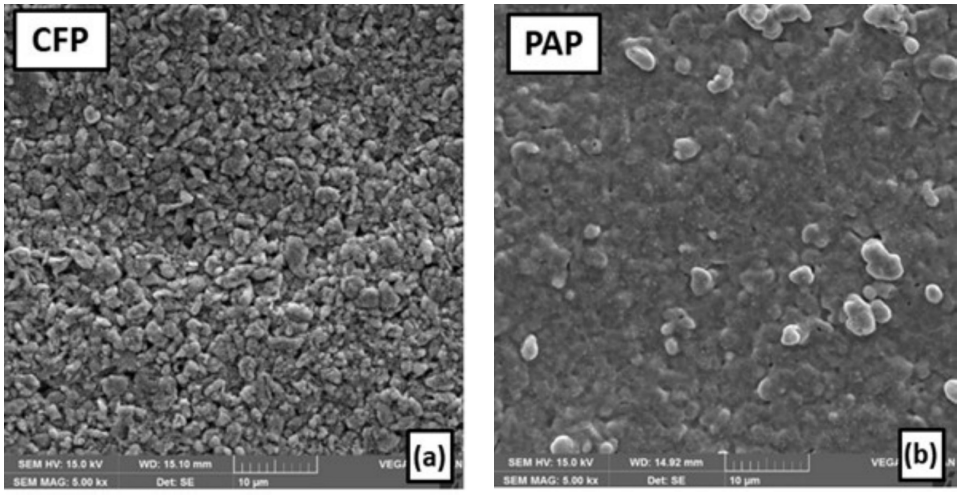

Figure 4. SEM micrographs of the coating surface after (a) CFP, (b) PAP at 1000 ˚C, acquired with secondary electrons.

Figure 5 shows the coating cross-sectional microstructures after pyrolysis at 1000 ˚C for 1 h, performed conventionally in Figure 5(a) and assisted by plasma in Figure 5(b). Regardless of the processing route, CFP or PAP, both samples presented a reaction zone (indicated in Figure 5 by the dotted yellow lines) in the coating/substrate interface. The cross-section of the PDC layers of both samples were similar in terms of porosity. However, after the process via PAP (Figure 5(b)) it is possible to notice that the Cr particles are more coalesced. Another observed difference between samples is that the reaction zone developed at the PDC/substrate layer interface is larger for samples processed via PAP (Figure 5(b)). Chemical analyses carried out in this region, for both samples as indicated by the numbered points in the figures, demonstrated the presence of Cr and C, in addition to the expected presence of Fe. Based on the composition of this region and the microstructural aspect, the formation of mixed carbides of the type $(Fe,Cr)_xC_y$ possibly occurred. The presence of nitrogen in the interface zone (between the PDC coating and the substrate), was detected in concentrations ranging from 2.5 to 4.5 wt.% for region 1 indicated in Figure 5(a) and (b)). In regions close to the surface of the coating, in the first micrometers, the nitrogen content reached up to 30.0 wt.%. The results provided by EDS in Figures 5(a) and 5(b) indicated the diffusion phenomenon occurring on two fronts, from the PDC coating towards the substrate and in the opposite direction. These results show that atoms from the coating, such as Cr and C, have migrated to the metal substrate, as well from the substrate to the coating as Fe, possibly related to resultant chemical concentration gradients influencing preferential diffusion among species. This interdiffusion between the coating and the steel substrate can be an indicator of good adhesion, which is extremely important for performance. Also, a diffusion layer is related as an additional protection against corrosion and oxidation in PDC coatings, as reported by Torrey and Bordia (2008).

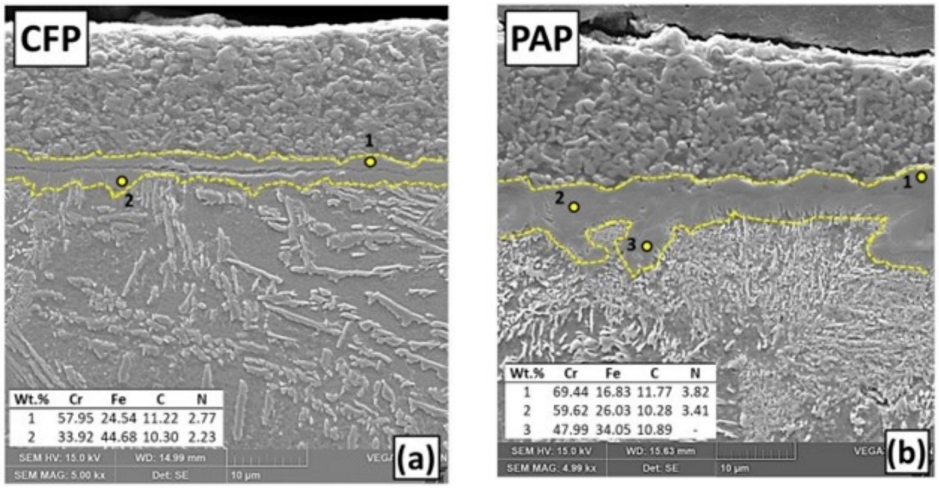

Figure 5. SEM micrographs of the cross-section of the coatings after (a) CFP, (b) PAP at 1000 ˚C, acquired with secondary electrons.

4. CONCLUSIONS

The pyrolysis of coatings with active Cr particles showed different conversion products according to the process. Comparatively, XRD analyses indicated that a small amount of the original Cr filler particles still remains unreacted after pyrolysis in a conventional furnace. Both nitride phases, CrN and Cr_2N, are present in the surface region of the coatings, but in the PAP process, the predominant phase is Cr_2N. In CFP, qualitatively both nitride phases showed similar proportions. The surface of the coatings after processing in CFP and PAP showed notable differences. When in PAP, the surface showed less porosity and higher coalescence between particles compared to CFP. In the analysis of the cross-section of the coatings, the porosity is quite similar between the two coatings. There seems to be a higher coalescing of the active Cr particles after the PAP process. Interdiffusion between coating and substrate was detected at the coating/substrate interface with the formation of a reaction zone in this region. In samples processed via PAP, this transformation zone was thicker than in samples processed in CFP.

One can say that by an appropriate choice of the system, precursor, active fillers, and plasma-assisted pyrolysis process parameters, it is possible to obtain coatings with tailored properties and compositions.

5. ACKNOWLEDGEMENTS

This research was financially supported by the Brazilian agencies CNPq, CAPES, BNDES, the Human Resources Program of the National Agency of Petroleum, Natural Gas and Biofuels – PRH-ANP/FINEP and DFG (German Research Foundation).

We thank Dr. rer. nat. habil. Günter Motz, head of the Polymer Derived Ceramics work group at the Ceramic Materials Engineering institute at the Universität Bayreuth, for providing the lab floor and equipment used to develop the CrSiCN coatings and for the discussions related to the PDC technology, during the Bragecrim collaboration.

6. REFERENCES

Cai, F., Yang, Q., Huang, X., Wei, R., 2010 Microstructure and Corrosion Behavior of CrN and CrSiCN Coatings. Journal Of Materials Engineering And Performance, v. 19, n. 5, p.721-727, http://dx.doi.org/10.1007/s11665-009-9534-3.

Cai, F.; Huang, X.; Yang, Q. 2015 Mechanical properties, sliding wear and solid particle erosion behaviors of plasma enhanced magnetron sputtering CrSiCN coating systems. Wear, v. 324-325, p.27-35. Elsevier BV. http://dx.doi.org/10.1016/j.wear.2014.11.008.

Chapman, B., Glow discharge processes. John Wiley & Sons, Inc., (USA) 1980, p. 406

Colombo, P., Mera, G., Riedel, R., Sorarù, G. D., 2010 Polymer-Derived Ceramics: 40 Years of Research and Innovation in Advanced Ceramics. Journal Of The American Ceramic Society, p.1805-1837. http://dx.doi.org/10.1111/j.1551-2916.2010.03876.x.

Flores, O., Schmalz, T., Krenkel, W., Heymann, L., Motz, G.. 2013 Selective cross-linking of oligosilazanes to tailored meltable polysilazanes for the processing of ceramic SiCN fibres. Journal Of Materials Chemistry A, v. 1, n. 48, p.15406-15415. http://dx.doi.org/10.1039/c3ta13254d.

Gilewicz, A., Chmielewska, P., Murzynski, D., Dobruchowska, E., Warcholinski, B., 2016, Corrosion resistance of CrN and CrCN/CrN coatings deposited using cathodic arc evaporation in Ringer's and Hank's solutions. Surface And Coatings Technology, v. 299, p.7-14. http://dx.doi.org/10.1016/j.surfcoat.2016.04.069.

Greil, P., 1995, Active-Filler-Controlled Pyrolysis of Preceramic Polymers. Journal Of The American Ceramic Society, v. 78, n. 4, p.835-848, http://dx.doi.org/10.1111/j.1151-2916.1995.tb08404.x

Hatakeyama, M., Tsuchiya, T., Lee, S., Matsuda, K., Aoi, Y., Nose, M., 2022, Influence of Iron Diffusion on the Oxidation Resistance of CrSiCN Hard Coatings. Materials Transactions, Vol. 63, No. 4, pp. 422 to 429. https://doi.org/10.2320/matertrans.MT-MA2022014.

Lin, J. Wang, B., Ou, Y., Sproul, W. D., Dahan, I., Moore, J. J., 2013, Structure and properties of CrSiN nanocomposite coatings deposited by hybrid modulated pulsed power and pulsed dc magnetron sputtering. Surface And Coatings Technology, v. 216, p.251-258. http://dx.doi.org/10.1016/j.surfcoat.2012.11.053.

Lin, J., Jang, J., Park, I., Wei, R., 2016, Structure and properties of CrSiCN coatings deposited by pulsed dc magnetron sputtering for wear and erosion protection. Surface And Coatings Technology, v. 287, p.44-54. http://dx.doi.org/10.1016/j.surfcoat.2015.12.068.

Martins, N., Bendo, T., Seifert, M., Medeiros, a., Gonçalves, P. C., Justus, T., De Lima, J. C., Motz, G., Klein, A. N., 2020, Plasma assisted pyrolysis for processing of composite ceramic coatings based on silazane precursor and TiB_2 filler applied onto a sintered steel. Open Ceramics, Vol 4, 100036. https://doi.org/10.1016/j.oceram.2020.100036.

Motz, G; Schmidt, S.; Beyer, S. 2008, The PIP - process: Precursor Properties and Applications. In: KRENKEL, W. (Ed.). Ceramic Matrix Composites: Fiber Reinforced Ceramics and their Applications. Germany: Wiley-VCH Verlag GmbH & Co. KGaA, 2008. Chapter 7. p. 165-186.

Riedel, R., Mera, G., Hauser, R., Klonczynski, A., 2006, Silicon-Based Polymer-Derived Ceramics: Synthesis Properties and Applications - A Review. Journal of the Ceramic Society of Japan, v. 114, n. 1330, p.425-444. http://dx.doi.org/10.2109/jcersj.114.425.

Šajgalík, P., Lencéš, Z., Hnatko, M. 2010 Nitrides. In Riedel, R.; Chen, I-W. (Ed.). Ceramics Science and Technology: Volume 2: Properties. WILEY-VCH Verlag GmbH & Co. KGaA, (Germany). 2010 Chapter 2, pages 59-89.

Seifert, M., Gonçalves, P., Justus, T., Martins, N., Klein, A. N., Motz, G. 2016, A novel approach to develop composite ceramics based on active filler loaded precursor employing plasma assisted pyrolysis, Materials & Design, v. 89, p. 893-900, https://doi.org/10.1016/j.matdes.2015.10.057 .

Torrey, J.D. Bordia, R.K. 2008, Processing of polymer-derived ceramic composite coatings on steel, Journal of the American Ceramic Society, v. 91, p. 41–45, https://doi.org/10.1111/j.1551- 2916.2007.02019.x .

Wang, Q., Wu, Z., Zhou, F., Huang, H., Niitzu, K., Yan, J.. 2015a, Evaluation of crack resistance of CrSiCN coatings as a function of Si concentration via nanoindentation. Surface And Coatings Technology, v. 272, p.239-245. http://dx.doi.org/10.1016/j.surfcoat.2015.04.001 .

Wang, Q., Wu, Z., Zhou, F., Yan, J.. 2015b, Comparison of crack resistance between ternary CrSiC and quaternary CrSiCN coatings via nanoindentation. Materials Science and Engineering: A, v. 642, p.391-397. http://dx.doi.org/10.1016/j.msea.2015.07.024.

Wang, Q., Zhou, F., Zhu, L., Zhang, M., Kong, J., 2019, Mechanical and tribological evaluation of CrSiCN, CrBCN and CrSiBCN coatings. Tribology International 130 146–154; https://doi.org/10.1016/j.triboint.2018.09.025

Wierzchoń, T; Ulbin-Pokorska, I; Sikorski, K. 2000, **Corrosion resistance of chromium nitride and oxynitride layers produced under glow discharge conditions.** Surface And Coatings Technology, v. 130, n. 2-3, p.274-279. http://dx.doi.org/10.1016/s0257-8972(00)00696-4.

Wu, Z., Zhou, F., Ma, Q., Wang, Q., Zhou, Z., Li, L., K.. 2016, Tribological and electrochemical properties of Cr–Si–C–N coatings in artificial seawater. RSC Advances, v. 6, n. 80, p.76724-76735. http://dx.doi.org/10.1039/c6ra19243b .

7. RESPONSIBILITY NOTICE

The authors are the only responsible for the printed material included in this paper.